

- 12) **Otsuka M, Oguni H, Liang JS et al:** STXBP1 mutations cause not only Ohtahara syndrome but also West syndrome—result of Japanese cohort study. *Epilepsia* **51**: 2449–2452, 2010
- 13) **Aicardi J:** Aicardi syndrome. *Brain Dev* **27**: 164–171, 2005
- 14) **Watanabe K, Negoro T, Aso K et al:** Reappraisal of interictal electroencephalograms in infantile spasms. *Epilepsia* **34**: 679–685, 1993
- 15) **Lux AL:** Is hypsarrhythmia a form of non-convulsive status epilepticus in infants? *Acta Neurol Scand* **115**: 37–44, 2007
- 16) **Vigevano F, Fusco L, Pachatz C:** Neurophysiology of spasms. *Brain Dev* **23**: 467–472, 2001
- 17) **Dulac O, Bast T, Dalla Bernardina B et al:** Infantile spasms: toward a selective diagnostic and therapeutic approach. *Epilepsia* **51**: 2218–2219; author reply 2221, 2010
- 18) **Yanagaki S, Oguni H, Yoshii K et al:** Zonisamide for West syndrome: a comparison of clinical responses among different titration rate. *Brain Dev* **27**: 286–290, 2005
- 19) **Frost JD, Hrachovy RA:** Infantile spasms: diagnosis, management and prognosis. Kluwer Academic Publishers, Boston (2003)
- 20) **Oguni H, Yanagaki S, Hayashi K et al:** Extremely low-dose ACTH step-up protocol for West syndrome: maximum therapeutic effect with minimal side effects. *Brain Dev* **28**: 8–13, 2006
- 21) **Yanagaki S, Oguni H, Hayashi K et al:** A comparative study of high-dose and low-dose ACTH therapy for West syndrome. *Brain Dev* **21**: 461–467, 1999
- 22) **Chugani HT, Asano E, Sood S:** Infantile spasms: who are the ideal surgical candidates? *Epilepsia* **51** (Suppl 1): 94–96, 2010
- 23) **Autry AR, Trevathan E, Van Naarden Braun K et al:** Increased risk of death among children with Lennox-Gastaut syndrome and infantile spasms. *J Child Neurol* **25**: 441–447, 2010
- 24) **小国弘量:** 【てんかんの診断と連携—プライマリ・ケア医に求められるてんかん診療—】 どのような場合に小児神経科専門医に紹介すべきか? *治療* **94**: 1703–1708, 2012
- 25) **Chellamuthu P, Sharma S, Jain P et al:** High dose (4 mg/kg/day) versus usual dose (2 mg/kg/day) oral prednisolone for treatment of infantile spasms: an open-label, randomized controlled trial. *Epilepsy Res* **108**: 1378–1384, 2014
- 26) **Arya R, Shinnar S, Glauser TA:** Corticosteroids for the treatment of infantile spasms: a systematic review. *J Child Neurol* **27**: 1284–1288, 2012
- 27) **Eun SH, Kang HC, Kim DW et al:** Ketogenic diet for treatment of infantile spasms. *Brain Dev* **28**: 566–571, 2006
- 28) **Hong AM, Turner Z, Hamdy RF et al:** Infantile spasms treated with the ketogenic diet: prospective single-center experience in 104 consecutive infants. *Epilepsia* **51**: 1403–1407, 2010
- 29) **Hirano Y, Oguni H, Shiota M et al:** Ketogenic diet therapy can improve ACTH-resistant West syndrome in Japan. *Brain Dev* **37**: 18–22, 2015
- 30) **伊藤 進, 小国弘量:** 【てんかんの新しい治療】小児難治性てんかんに対するケトン食療法 「最後の選択肢」から「早期からの選択肢」へ. *Brain Nerve* **63**: 393–400, 2011
- 31) **Vining EP, Freeman JM, Ballaban-Gil K et al:** A multicenter study of the efficacy of the ketogenic diet. *Arch Neurol* **55**: 1433–1437, 1998
- 32) **Parmar MS:** Kidney stones, carbonic anhydrase inhibitors, and the ketogenic diet. *Epilepsia* **44**: 735, 2003
- 33) **Neal EG, Chaffe H, Schwartz RH et al:** The ketogenic diet for the treatment of childhood epilepsy: a randomised controlled trial. *Lancet Neurol* **7**: 500–506, 2008
- 34) **Shewmon D, Shields W, Sankar R et al:** Follow-up on infants with surgery for catastrophic epilepsy. *In Paediatric epilepsy syndromes and their surgical treatment* (Tuxhorn I, Holthausen H, Boenigk H eds), pp513–525 (1997)
- 35) **Jonas R, Asarnow RF, LoPresti C et al:** Surgery for symptomatic infant-onset epileptic encephalopathy with and without infantile spasms. *Neurology* **64**: 746–750, 2005
- 36) **Baba H:** Surgical and developmental outcome after callosotomy for West syndrome without resectable MRI lesion: Surgical timing and prevention of developmental delay. *In International Symposium on Surgery for Catastrophic Epilepsy in Infants* (ISCE), The 14th annual meeting of ISS: 92 (2012)
- 37) **Fujii A, Oguni H, Hirano Y et al:** A long-term, clinical study on symptomatic infantile spasms with focal features. *Brain Dev* **35**: 379–385, 2013

## 2. 各種疾患における診療目的の遺伝学的検査

### 3) 先天代謝異常症におけるタンデムマスと遺伝学的検査の併用

高柳正樹

タンデム型質量分析計を用いる測定法であるタンデムマススペクトロメトリーは、先天性代謝疾患の診断において有力な診断手段である。先天性代謝異常症の診断においては、アミノ酸はニュートラルロススキャン分析法、アシルカルニチンはプリカーサーイオンスキャン分析が用いられている。タンデムマスで発見された症例の確定疾患へのステップとして、遺伝学的検査（酵素学的検討、遺伝子検査）が行われる。一部疾患に対しては保険が適応されている。遺伝学的検査の依頼先としては日本先天代謝異常学会ホームページやNPO法人オーファンネットジャパンホームページを参考にする。

#### はじめに

タンデム型質量分析計を用いる測定法であるタンデムマススペクトロメトリーが、先天性代謝疾患の診断において有力な診断手段になることが、Millingtonら<sup>1)</sup>により提言されはじめてからすでに30年近くになる。タンデムマススペクトロメトリーの技術は先天性代謝異常症のみならず、あらゆる物質の同定や定量に応用され、特に薬毒物分析や法医学分野で発展が目覚ましい。この検査法は測定が短時間で可能であることから、極めて多くの検体を処理しなければならない新生児マススクリーニングへの応用が検討され、現在では世界中で広くタンデムマススペクトロメトリーによる先天性代謝疾患のスクリーニングが行われている。

タンデム型質量分析計は略してタンデムマスと

呼ばれることが多い。さらに、それを用いるタンデムマススペクトロメトリーもタンデムマスと呼ばれる。上に述べたように新生児マススクリーニングにも応用されていることから、新生児マススクリーニングもタンデムマスと呼ばれることもあり、用語の意味については注意が必要である。

#### I. タンデムマススペクトロメトリーの簡単な原理

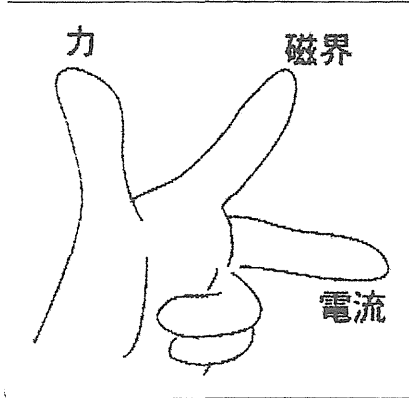
タンデムマススペクトロメトリーは基本的には質量分析器<sup>用語1)</sup>を2台連結して使用するシステムである。質量分析器は磁力、電流、力の関係（フレミングの左手の法則、図①）を利用して、物質の質量を測定する機器である。図②にタンデム型質量分析計の写真を<sup>2)</sup>、図③にその構造のシェーマを示した<sup>3)</sup>。詳細な測定法の解説は省略する。

#### key words

タンデム型質量分析計, 拡大新生児マススクリーニング, アシルカルニチン一斉分析, 遺伝学的検査, 有機酸代謝異常症, 脂肪酸代謝異常症, 先天性銅代謝異常症, アミノ酸代謝異常症, 保険診療報酬

先天性代謝異常症の診断においては、アミノ酸の一斉分析にはニュートラルロスキャン分析法、アシルカルニチン一斉分析にはプリカーサーイオンスキャン分析が用いられている。アシルカルニチン一斉分析により、検体中の各種アシルカ

ルニチン<sup>4)</sup>の同定・定量を1検体数分で行うことができる。それぞれの先天性代謝異常症（ことに有機酸代謝異常症、脂肪酸代謝異常症）においては特異的なアシルカルニチンの蓄積が認められることから、タンデムマスにより診断が可能になる。



図① フレミングの左手の法則

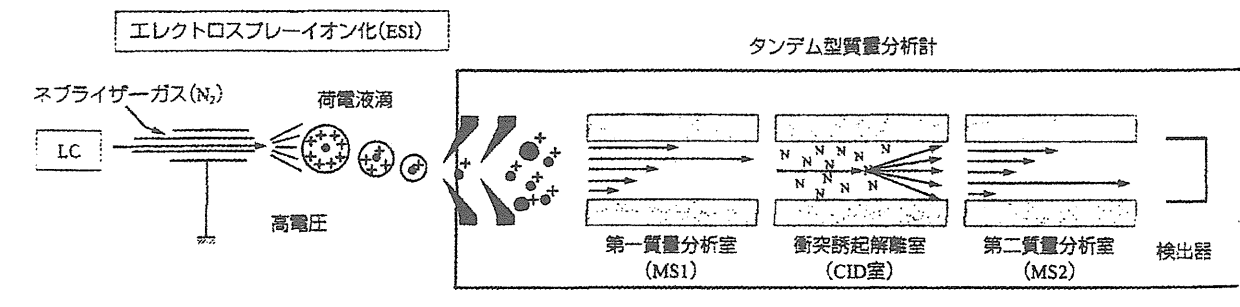
図④に血液濾紙を用いた中鎖アシル CoA 脱水素酵素欠損症症例のタンデムマスによる結果を示した<sup>4)</sup>。横軸はアシルカルニチンの質量数、縦軸はその量を示す。C8のアシルカルニチン(octenoylcarnitine)などが異常高値を示し、上記診断が疑われることになった。

## II. 「先天代謝異常症などに関する新生児マススクリーニング」の成果

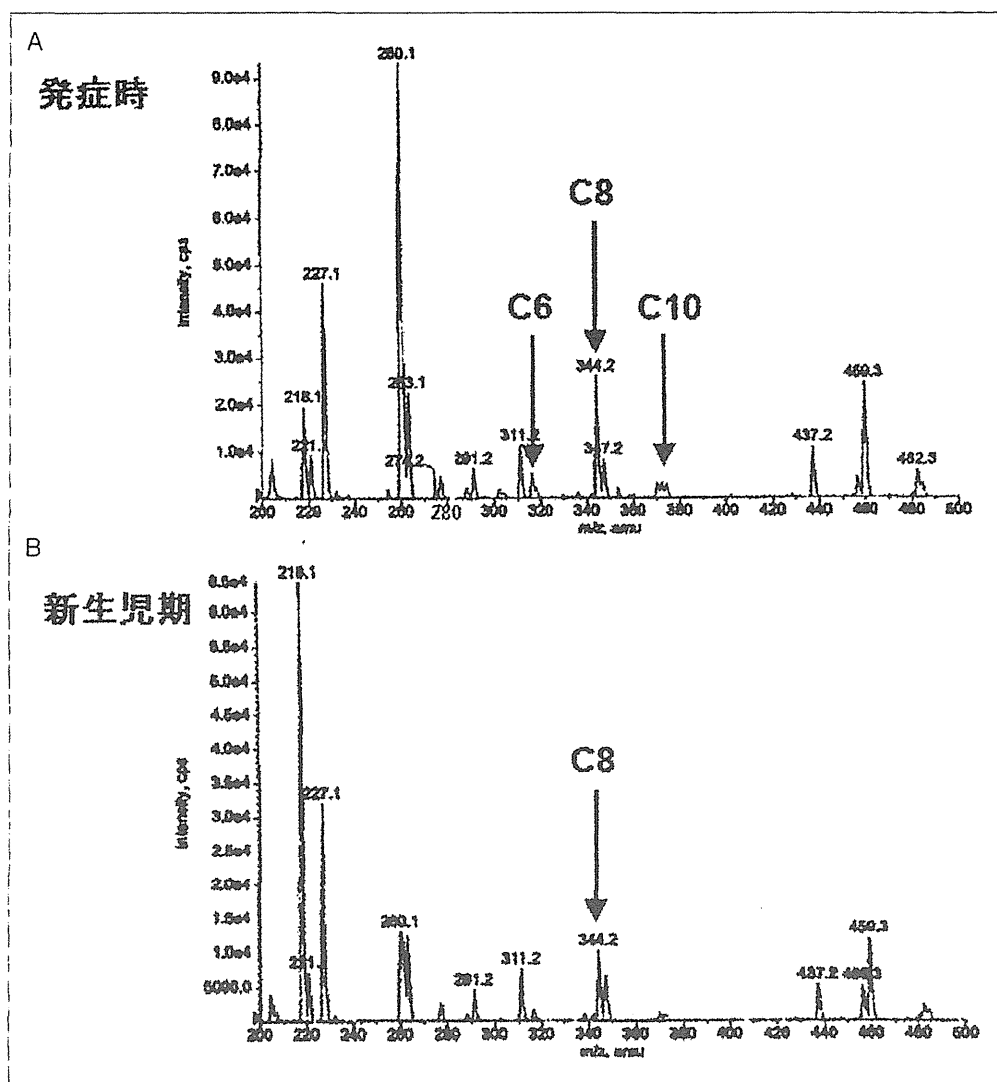
タンデムマスの最大の成果は新生児代謝異常マススクリーニングと考えられるので、簡単にそ



図② タンデム型質量分析計 (文献2より)



図③ タンデム型質量分析計の構造 (文献3より)



図④ 中鎖アシル CoA 脱水素酵素欠損症症例のアシルカルニチン分析 (文献 4 より)

- A. 発症時濾紙血のアシルカルニチン分析にて C8 の上昇を認め、MCAD 欠損症が示唆された。  
 B. 新生児期濾紙血の分析でも C8 の上昇を認めた。

の内容を説明する。タンデムマスを用いたスクリーニングは、拡大新生児マススクリーニング、Expanded Neonatal Mass-screening またはタンデムマス (マススクリーニング) と呼ばれている。

新生児マススクリーニングは日本医学会の「医療における遺伝学的検査・診断に関するガイドライン」にも、明確にこのガイドラインの適応範囲であるとされている。したがって、この検査を受けるにあたっての同意の取得に関しては、十分な方法がとられるべきであるという意見がある。

表①に現在日本で行われている新生児代謝異常マススクリーニングにおいてタンデムマスによっ

て測定されている疾患の一覧を示す。アミ枠内はその疾患発見感度や発見後の有効な治療法の問題から、セカンドラインの対象疾患として考えられている疾患である。

表②に、これまで発見された患者数を示す。約 9 千人に 1 人の割合で患者が発見されている<sup>5)</sup>。特に以前は日本には存在しないとされていた先天性脂肪酸代謝異常症が多く発見されていることは特記すべきことと思われる。

タンデムマススクリーニングに関しては NPO のタンデムマス・スクリーニング普及協会が設立されている。タンデムマス検査の依頼 (有料) や

表① 拡大新生児マススクリーニングにおいてタンデムマスで診断されている疾患一覧

脂肪酸代謝異常症	
CPT I 欠損症	5
CPT II 欠損症	7
VLCAD 欠損症	12
MCAD 欠損症	18
グルタル酸尿症 II 型	6
その他も含め	57
有機酸代謝異常症	
メチルマロン酸血症	18
プロピオン酸血症	43
イソ吉草酸血症	3
複合カルボキシラーゼ欠損症	3
3MCC 欠損症	13
グルタル酸尿症 I 型	7
その他も含め	86
アミノ酸代謝異常症	
フェニルケトン尿症	37
シトリン欠損症	23
アルギニノコハク酸尿症	2
その他も含め	72
計	215
スクリーニング数	1949987

スクリーニングの結果についての疑問などについては、ここに問い合わせるのがよいと考えられる

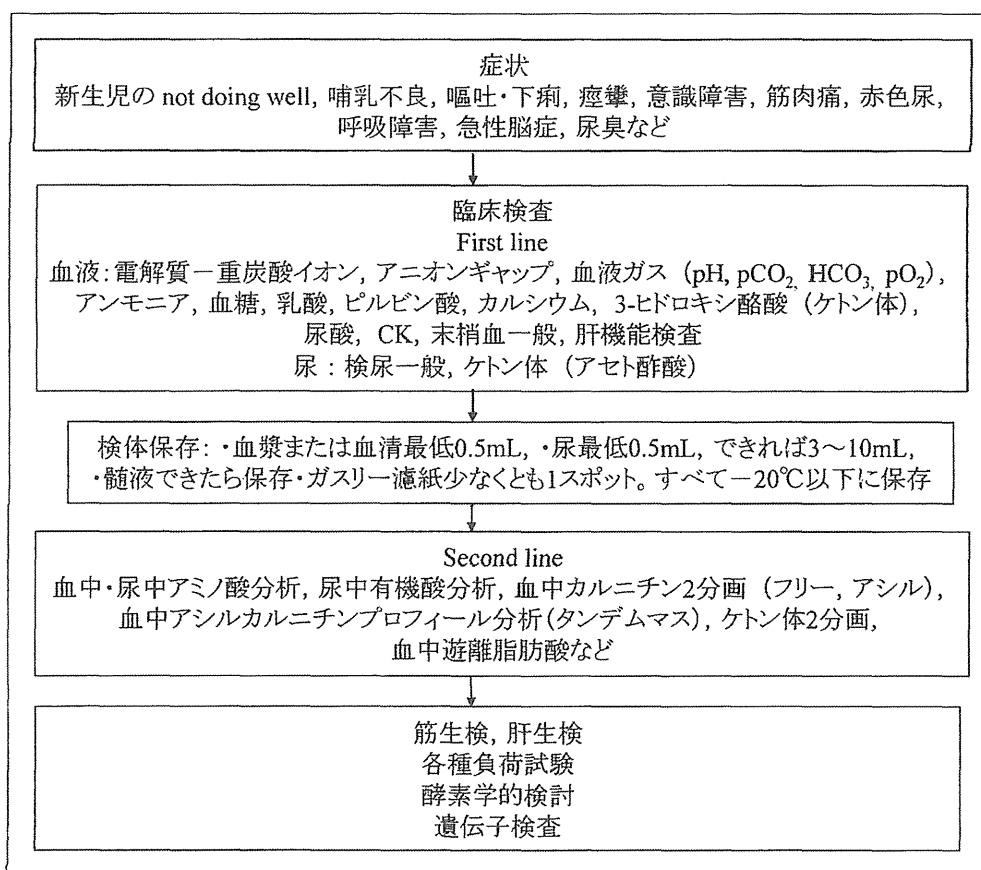
### Ⅲ. 先天性代謝異常症の診断の流れ-タンデムマスと遺伝子(遺伝学的)検査の位置づけ-

先天性代謝異常症の症状は、嘔吐、痙攣、意識障害など非特異的なものが多い。代謝異常症を見逃さないためには、あらかじめ「まず」最初に行う検査 (first line) を決めておき、それら検査の結果で「次に」行う検査を (second line) 考えることが重要である<sup>61)</sup>。この流れを図示したものが図⑤である。

タンデムマスは second line の検査として考えられている検査である。現在、新生児マススクリーニングにて広く実施されているので、検査としてはアクセスが非常に容易になっている。アミノ酸分析や有機酸分析などの検査などから、高い精度で診断が考えられるときには筋生検、肝生検、各種負荷試験、酵素学的検討、遺伝子検査へと診断を進めることになる。

表② これまで拡大新生児マススクリーニングにおいて発見された先天性代謝異常症患者一覧 (文献5より)

〔有機酸代謝異常症〕	
(1) メチルマロン酸血症	(約 8 万人に 1 人)
(2) プロピオン酸血症	(約 3 万人に 1 人)
(3) $\beta$ ケトチオラーゼ欠損症	(非常に稀な疾患)
(4) イソ吉草酸血症	(約 100 万人に 1 人)
(5) メチルクロトニルグリシン尿症	(非常に稀な疾患)
(6) ヒドロキシメチルグルタル酸血症	(非常に稀な疾患)
(7) マルチプルカルボキシラーゼ欠損症	(約 20 万人に 1 人)
(8) グルタル酸血症 I 型	(約 8 万人に 1 人)
〔脂肪酸代謝異常症〕	
(9) 中鎖アシル CoA 脱水素酵素 (MCAD) 欠損症	(約 8 万人に 1 人)
(10) 極長鎖アシル CoA 脱水素酵素 (VLCAD) 欠損症	(約 20 万人に 1 人)
(11) 三頭酵素 (TFP) 欠損症 / 長鎖 3-ヒドロキシアシル CoA 脱水素酵素 (LCHAD) 欠損症	(非常に稀な疾患)
(12) カルニチンパルミトイルトランスフェラーゼ 1 (CPT1) 欠損症	(約 20 万人に 1 人)
(13) カルニチンパルミトイルトランスフェラーゼ 2 (CPT2) 欠損症	(約 20 万人に 1 人)
(14) カルニチンアシルカルニチントランスロカーゼ欠損症	(非常に稀な疾患)
(15) 全身性カルニチン欠乏症 (カルニチントランスポーター異常症)	(約 4 万人に 1 人)
(16) グルタル酸血症 2 型	(約 10 万人に 1 人)
〔尿素サイクル異常症〕	
(17) シトルリン血症 I 型 (アルギニノコハク酸合成酵素欠損症)	(非常に稀な疾患)
(18) アルギニノコハク酸尿症 (アルギニノコハク酸リアーゼ欠損症)	(約 20 万人に 1 人)



図⑤ 代謝性疾患の診断の流れ

#### IV. 先天性代謝異常症における遺伝学的検査および遺伝カウンセリングの保険上の取り扱い

平成 24 年 (2012 年) 度に行われた保険診療報酬改定で, 遺伝学的検査が行える先天性代謝異常症に新生児マススクリーニング対象疾患が多く追加された (表③)。なお, この検査は患者 1 人につき 1 回だけ 3880 点, つまり患者の一生に 1 回だけ算定できる。

検査の実施にあたっては, 厚生労働省「医療・介護関係事業者における個人情報の適切な取扱いのためのガイドライン」(平成 16 年 12 月) および関係学会による「遺伝学的検査に関するガイドライン」(平成 15 年 8 月) を遵守することが指示されている。

遺伝カウンセリングは, 遺伝カウンセリング加算の施設基準を満足し, 当局に申請認可されてい

表③ 遺伝学的検査が適応される先天性代謝疾患一覧

ムコ多糖症 I 型, ムコ多糖症 II 型, ゴーシェ病, ファブリ病, ボンベ病, フェニルケトン尿症, メーブルシロップ尿症, ホモシスチン尿症, シトルリン血症 (I 型), アルギニノコハク酸血症, メチルマロン酸血症, プロピオン酸血症, イソ吉草酸血症, メチルクロトニルグリシン血症, HMG 血症, 複合カルボキシラーゼ血症, グルタル酸血症 I 型, MCDA 欠損症, VLCAD 欠損症, MTP (LCHAD) 欠損症, CPT1 欠損症, 先天性銅代謝異常症 (メンケス病やウィルソン病) など

る施設において, 患者またはその家族に対し遺伝学的検査の結果に基づき, 遺伝カウンセリングを行った場合に月に 1 回算定できるとされている。以下に遺伝カウンセリング加算の施設基準を示す。

①当該保険医療機関内に遺伝カウンセリングを要する治療に係る十分な経験を有する常勤の医師

が配置されていること

- ②当該カウンセリングを受けたすべての患者またはその家族に対して、それぞれの患者が受けたカウンセリングの内容が文書により交付され、説明がなされていること

## V. 遺伝学的検査（酵素学的検討、遺伝子検査）の実際

タンデムマスで発見された症例の確定診断へのステップとしての酵素学的検討、遺伝子検査が行われるが、日本国内では検査実施施設をすべての疾患で探し出すのは困難である。ことに酵素学的検査は他の分野と同様に行われている施設は極めて少なく、簡単に依頼できる状況にはない。遺伝子検査も同様な状況にあるが、次世代シーケンサーなどの遺伝子解析の技術の進歩に伴うパラダイムシフトが起きつつある。しかし現状では、安定した先天性代謝異常症に対する遺伝子検査の供給システムが整っているとは考えられない。不十分な供給システムではあるが、遺伝子検査が必要と考えられるときには、日本先天代謝異常学会のホームページにアップされている精密検査施設（連絡先）と対象疾患をチェックするのが良いと考えられる。また NPO 法人 オーファンネット

ジャパンでも先天性代謝異常症の遺伝子検査の供給（有料）を行っているので、こちらもチェックしていただきたい。

保険収載されていない疾患においてはもちろんだが、保険収載されている場合でも検査料金が1万円以上であるときには、遺伝子検査費用を誰が負担するかについての議論が残る。

遺伝子検査の結果を保因者診断や出生前診断などに使用する際には、代謝異常疾患以外の多くの分野でも検討されている課題についての十分な検討が必要である。

## おわりに

私は、先天性代謝異常症の診療において、この30年間の最もエポックメイキングなことは、酵素補充療法と並んでこのタンデムマスの臨床応用の開発であると考えている。

先天性代謝異常症において遺伝子検査が、患者の診療、特にその治療を大きく変えたということはないと私は考えている。しかし次世代シーケンサーの臨床への応用が進めば、タンデムマスと組み合わせた全く新しい診療体制が作り出されることが可能性は大きいと思われる。

### 用語解説

1. 質量分析器：フレミングの左手の法則により、磁場をかけることにより荷電している物質に力を発生させる。質量が大きければ曲がりが少ないことを利用して、物質の質量を測定する機器である。
2. アシルカルニチン：脂肪酸とカルニチンのエステルで

ある。正常の脂肪酸の酸化代謝経路にも発生する謝障害があった場合に蓄積する異常代謝産物がカルニチンと結合して解毒されることもある。いかなるアシルカルニチンが体内に蓄積しているかがわかれば、謝障害の部位がわかる。

### 参考文献

- 1) Millington DS, Maltby DA, et al : Clin Chim Acta 16, 173-178, 1986.
- 2) タンデムマス・スクリーニング情報－福井大学ホームページ  
<http://www.med.u-fukui.ac.jp/shouni/Screening/ScrOA.html>
- 3) 山口清次：タンデムマスの原理 タンデムマス・スクリー

- ニング, 診断と治療社, 18-21, 2013.
- 4) 小林真之, 他：特殊ミルク情報 45, 7-9, 2009.
- 5) 山口清次：厚労省 平成 22-24 年度山口班研究班報告書, 3-17, 平成 25 年 5 月.
- 6) 藤浪綾子, 高柳正樹：小児科診療 69, 1574-1578, 2010.
- 7) 高柳正樹：代謝救急 見逃せない先天代謝異常 (三上嵐隆編), 2-4, 中山書店, 2011.

参考ホームページ

- ・タンデムマス・スクリーニング普及協会  
<http://tandem-ms.or.jp/>
- ・日本先天代謝異常学会  
<http://square.umin.ac.jp/JSIMD/>
- ・NPO 法人 オーファンネットジャパン  
<http://onj.jp/list/index.html>
- ・日本医学会の「医療における遺伝学的検査・診断に関するガイドライン」  
<http://jams.med.or.jp/guideline/genetics-diagnosis.html>

高柳正樹

- 1975年 金沢大学医学部卒業  
千葉大学医学部附属病院小児科
- 1976年 日本赤十字社医療センター小児科
- 1977年 千葉大学医学部附属病院小児科
- 1984年 医学博士（千葉大学 B）
- 1988年 千葉県こども病院小児科医長
- 2000年 同小児科部長
- 2005年 同医療局長
- 2011年 同副院長

第3章

生殖細胞系列遺伝学的検査の臨床応用



## Intra-mitochondrial Methylation Deficiency Due to Mutations in *SLC25A26*

Yoshihito Kishita,<sup>1,16</sup> Aleksandra Pajak,<sup>2,16</sup> Nikhita Ajit Bolar,<sup>3,16</sup> Carlo M.T. Marobbio,<sup>4,16</sup> Camilla Maffezzini,<sup>2</sup> Daniela V. Miniero,<sup>4</sup> Magnus Monné,<sup>4,5</sup> Masakazu Kohda,<sup>6</sup> Henrik Stranneheim,<sup>7,8</sup> Kei Murayama,<sup>9</sup> Karin Naess,<sup>7,10</sup> Nicole Lesko,<sup>7,10</sup> Helene Bruhn,<sup>7,10</sup> Arnaud Mourier,<sup>11</sup> Rolf Wibom,<sup>7,10</sup> Inger Nennesmo,<sup>12</sup> Ann Jespers,<sup>13</sup> Paul Govaert,<sup>13</sup> Akira Ohtake,<sup>14</sup> Lut Van Laer,<sup>3</sup> Bart L. Loeyls,<sup>3,15</sup> Christoph Freyer,<sup>2,7</sup> Ferdinando Palmieri,<sup>4,17,\*</sup> Anna Wredenberg,<sup>2,7,17,\*</sup> Yasushi Okazaki,<sup>1,6,17</sup> and Anna Wedell<sup>2,7,8,17</sup>

S-adenosylmethionine (SAM) is the predominant methyl group donor and has a large spectrum of target substrates. As such, it is essential for nearly all biological methylation reactions. SAM is synthesized by methionine adenosyltransferase from methionine and ATP in the cytoplasm and subsequently distributed throughout the different cellular compartments, including mitochondria, where methylation is mostly required for nucleic-acid modifications and respiratory-chain function. We report a syndrome in three families affected by reduced intra-mitochondrial methylation caused by recessive mutations in the gene encoding the only known mitochondrial SAM transporter, *SLC25A26*. Clinical findings ranged from neonatal mortality resulting from respiratory insufficiency and hydrops to childhood acute episodes of cardiopulmonary failure and slowly progressive muscle weakness. We show that *SLC25A26* mutations cause various mitochondrial defects, including those affecting RNA stability, protein modification, mitochondrial translation, and the biosynthesis of CoQ10 and lipoic acid.

Altered S-adenosylmethionine (SAM) concentrations in the cytoplasm have been suggested to be involved in the pathophysiology of disease and in the natural aging process.<sup>1,2</sup> Highly specialized methyltransferases, encoding approximately 1%–2% of eukaryotic genomes,<sup>3</sup> use SAM as a methyl group donor to methylate their targets. The human mitochondrial SAM carrier (SAMC), encoded by *SLC25A26* (MIM: 611037), is expressed in all human tissues examined and is believed to be the only route of SAM entry into mitochondria.<sup>4</sup> However, regulatory mechanisms of intra-mitochondrial SAM (mtSAM) concentrations or other pathways modulating mtSAM levels are unknown, and so far the pathophysiological consequences of reduced mitochondrial SAM import are unclear.

We identified three families with different ethnic origins and a complex biochemical phenotype caused by mutations in *SLC25A26*. Individual 1 (P1, individual II:2 from family 1 in Figure 1A) was born to consanguineous parents from Iraq and presented at 4 weeks with acute circulatory collapse and pulmonary hypertension, requiring

extra-corporeal membrane oxygenation for 5 days. He had severe lactic acidosis around 20 mmol/l (reference: 0.5–2.3). Sodium dichloroacetic acid had good effect, and the boy slowly normalized. At 3.5 years, he had a second episode of pulmonary hypertension, which also normalized. At 6 years 3 months, the boy had increasing muscle weakness, fatigue, recurrent abdominal pain, lack of appetite, and slightly delayed development. Investigation of mitochondrial function from a muscle biopsy revealed reduced activities of complexes I and IV and a reduced ATP production rate, in particular when pyruvate was used as a substrate (Figures S1A and S1B). Histology showed the presence of COX-negative muscle fibers (Figure S1C). Additionally, Blue-native PAGE (BN-PAGE) revealed reduced levels of assembled complexes I and IV (Figure S1D). Individual 2 (P2, II:1 from family 2 in Figure 1A), born to Japanese parents, developed severe lactic acidosis up to 42 mmol/l (reference: <1.8), an elevated pyruvate level (0.65 mmol/l; reference: <0.1), and respiratory failure 11 hr after birth, prompting mechanical

<sup>1</sup>Division of Functional Genomics & Systems Medicine, Research Center for Genomic Medicine, Saitama Medical University, 1397-1 Yamane, Hidaka-shi, Saitama 350-1241, Japan; <sup>2</sup>Max Planck Institute Biology of Ageing – Karolinska Institutet Laboratory, Division of Metabolic Diseases, Department of Laboratory Medicine, Karolinska Institutet, 171 77 Stockholm, Sweden; <sup>3</sup>Department of Medical Genetics, Faculty of Medicine and Health Sciences, Antwerp University Hospital, University of Antwerp, Antwerp 2650, Belgium; <sup>4</sup>Department of Biosciences, Biotechnologies and Biopharmaceutics, University of Bari, Via Edoardo Orabona 4, 70125 Bari, Italy; <sup>5</sup>Department of Sciences, University of Basilicata, Via Ateneo Lucano 10, 85100 Potenza, Italy; <sup>6</sup>Division of Translational Research, Research Center for Genomic Medicine, Saitama Medical University, 1397-1 Yamane, Hidaka-shi, Saitama 350-1241, Japan; <sup>7</sup>Centre for Inherited Metabolic Diseases, Karolinska University Hospital, 171 76 Stockholm, Sweden; <sup>8</sup>Science for Life Laboratory and Department of Molecular Medicine and Surgery, Karolinska Institutet, 171 76 Stockholm, Sweden; <sup>9</sup>Department of Metabolism, Chiba Children's Hospital, 579-1 Heta-cho, Midori, Chiba 266-0007, Japan; <sup>10</sup>Department of Laboratory Medicine, Karolinska Institutet, 171 77 Stockholm, Sweden; <sup>11</sup>Max Planck Institute for Biology of Ageing, 50931 Cologne, Germany; <sup>12</sup>Department of Pathology, Karolinska University Hospital, 171 77 Stockholm, Sweden; <sup>13</sup>Paola Children's Hospital, ZNA Middelheim, Antwerp 2650, Belgium; <sup>14</sup>Department of Pediatrics, Saitama Medical University, 38 Morohongo Moroyama-machi, Iruma-gun, Saitama 350-0495, Japan; <sup>15</sup>Department of Genetics, Radboud University Medical Center, Nijmegen, 6525 GA, the Netherlands

<sup>16</sup>These authors contributed equally to this work

<sup>17</sup>These authors contributed equally to this work

\*Correspondence: [ferdinando.palmieri@uniba.it](mailto:ferdinando.palmieri@uniba.it) (F.P.), [anna.wredenberg@ki.se](mailto:anna.wredenberg@ki.se) (A.W.)

<http://dx.doi.org/10.1016/j.ajhg.2015.09.013>. ©2015 The Authors

This is an open access article under the CC BY-NC-ND license (<http://creativecommons.org/licenses/by-nc-nd/4.0/>).

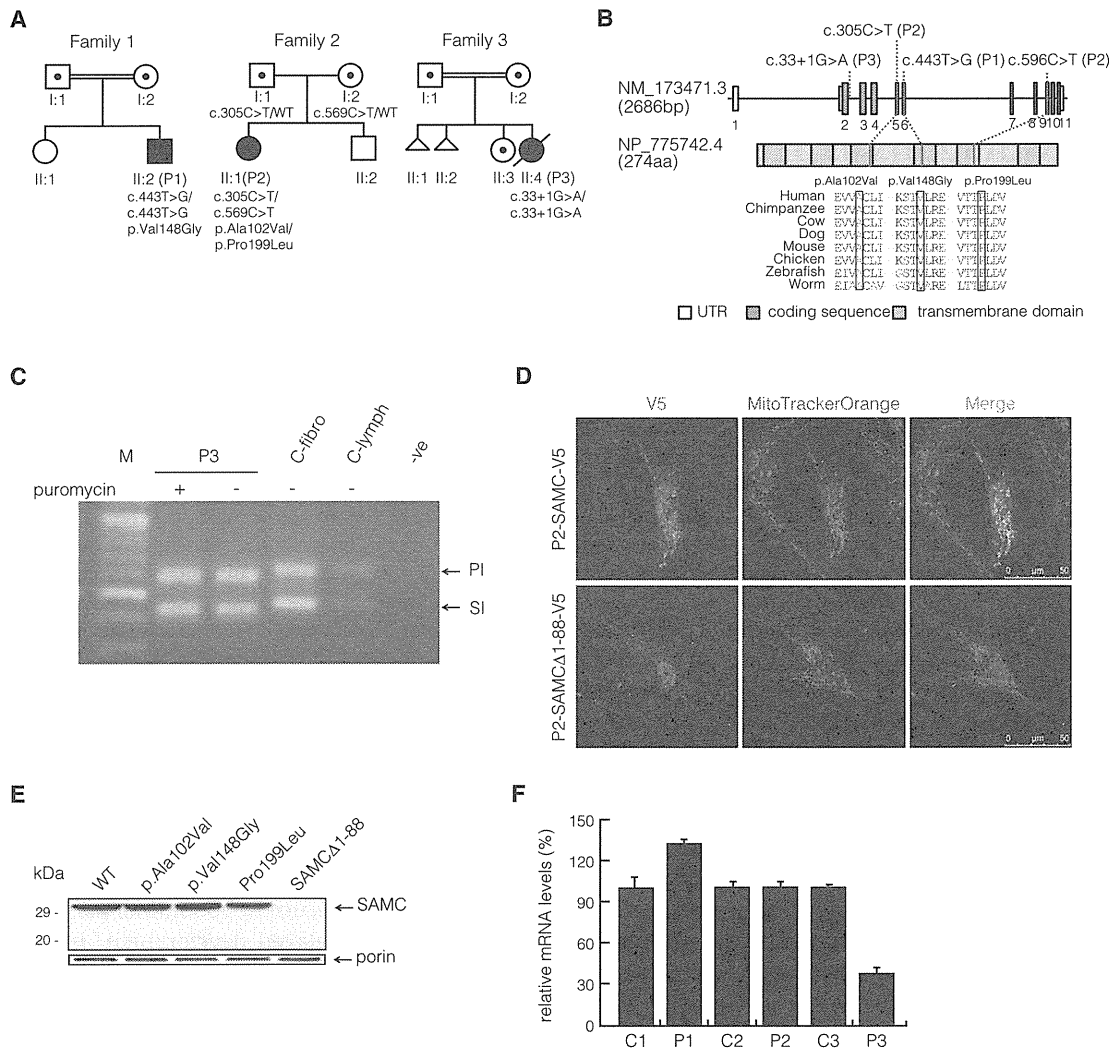


**Figure 1. Identification of Mutations in *SLC25A26***

(A) Pedigrees of individuals P1–P3 indicate the inheritance patterns in the individuals' families. P1 was born to consanguineous parents from Iraq after a normal pregnancy and neonatal period. P2 was born full term to unrelated parents from Japan with an Apgar score of 9–10. P3 was born to consanguineous parents of Moroccan descent. Symbols and colors are defined as follows: square, male; circle, female; triangle, miscarriage with unknown gender; white, unaffected; dot, unaffected carrier; black, affected. WT indicates wild-type. (B) Diagram representing the relative positions of *SLC25A26* mutations (NM\_173471.3) and *SLC25A26* alterations (GenBank: NP\_775742.4). Amino acid alignments of eight species show the regions of each mutation.

(C) *SLC25A26* mutation c.33+1G>A causes an RNA-splicing defect: the top band in lanes 2–5 indicates the amplification of the principal isoform (PI; Ensembl: ENST00000354883), and the lower band in lanes 2–5 indicates the amplification of the shorter isoform (SI; Ensembl: ENST00000336733). As a result of the mutation, PCR products from the individual, treated both with and without puromycin, were observed to be shorter in length (top band: PI around 572 bp; lower band: SI around 415 bp) than those of the control fibroblasts and lymphocytes (top band: PI 617 bp; lower band: SI 450 bp). No difference was observed between the puromycin-treated and non-puromycin-treated P3 samples. Lane contents are as follows: lanes 1 and 7, 100 bp DNA ladder (Fermentas); lane 2, PCR products amplified from cDNA extracted from P3 fibroblasts treated with puromycin; lane 3, PCR products amplified from cDNA extracted from P3 fibroblasts cultured without puromycin; lane 4, PCR products amplified from cDNA extracted from control fibroblasts; lane 5, PCR products amplified from cDNA extracted from control lymphocytes; and lane 6, PCR reaction blank.

(D) Subcellular localization of C-terminal V5-tagged SAMC (p2-SAMC-V5) and the shortened SAMCΔ1–88 (p2-SAMCΔ1–88) in P2 fibroblasts stained with MitoTrackerOrange.

(E) Amounts of wild-type (WT) SAMC, p.Ala102Val SAMC, p.Val148Gly SAMC, p.Pro199Leu SAMC, SAMCΔ1–88, and endogenous porin in mitochondria from SAM5Δ yeast transformed with WT SAMC-pYES2 (SAMC), p.Ala102Val SAMC-pYES2 (p.Ala102Val), p.Val148Gly SAMC-pYES2 (p.Val148Gly), p.Pro199Leu SAMC-pYES2 (p.Pro199Leu), and short SAMC-pYES2 (SAMCΔ1–88). Equal amounts of mitochondrial lysates (30 μg protein) were separated by SDS-PAGE, transferred to nitrocellulose, and immunodecorated with the anti-hemagglutinin or the anti-porin antibody.

(F) Relative *SLC25A26* mRNA steady-state levels in fibroblasts as determined by qRT-PCR. Values are normalized to 18S rRNA levels. Error bars show the SEM.

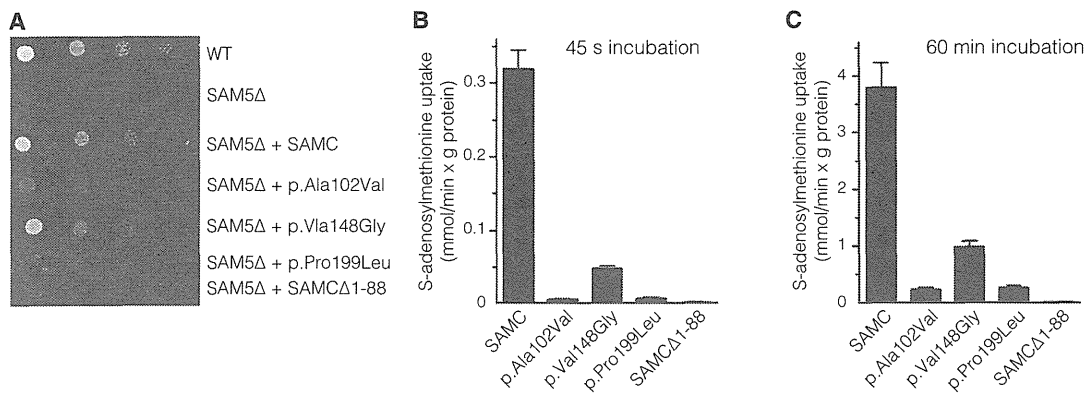


**Figure 2. In Vivo and In Vitro Pathology of the *SLC25A26* Mutations**

(A) 4-fold serial dilution of wild-type (WT) yeast cells, SAM5Δ cells, and SAM5Δ cells transformed with WT SAMC-pYES2 (SAMC), p.Ala102Val SAMC-pYES2 (p.Ala102Val), p.Val148Gly SAMC-pYES2 (p.Val148Gly), p.Pro199Leu SAMC-pYES2 (p.Pro199Leu), and short SAMC-pYES2 (SAMCΔ1–88) were plated on YP medium supplemented with 3% glycerol and 0.05% galactose for 72 hr at 30°C. (B and C) Liposomes reconstituted with WT or the indicated SAMC variants were preloaded with 10 mM S-adenosylmethionine at 25°C. Transport was started with 1 mM [<sup>3</sup>H]S-adenosylmethionine and terminated after (B) 45 s or (C) 60 min. The values are means ± SD of at least four independent experiments.

ventilation and dichloroacetic acid treatment. The child improved, and gross development was normal until 2 years of age, when she experienced an additional episode of severe lactic acidosis (36 mmol/l) followed by cardiopulmonary arrest and hypoxic brain damage. After this episode, the individual has remained severely handicapped. Activities of respiratory-chain enzymes were normal in fibroblasts but showed decreased activities of complexes I, III, and IV in skeletal muscle (Figure S1E). Muscle histology was normal at day 6 but revealed both ragged red fibers and COX-negative fibers when individual 2 was 3 years of age (Figure S1F). Individual 3 (P3, individual II:4 from family 3 in Figure 1A), born to consanguineous parents of Moroccan descent, was delivered by caesarean section at 30 weeks 5 days after reduced fetal movements, polyhydramnios, fetal hydrops, and poor cardiotocography (CTG) readings were noted from 27 weeks of gestational age. She had normal anthropometric parameters (birth weight 1,300 g, length 38 cm, and head circumference 27.5 cm) but presented with a poor Apgar score (3–5–6) due to bradycardia, hypotonia, and respiratory insufficiency, necessitating assisted ventilation with high-frequency oscillation. Urine lactate and pyruvate levels were 18 mmol/mmol creatinine (reference: 1–285 μmol/mmol creatinine) and 1.2 mmol/mmol creatinine (reference: 1–130 μmol/mmol creatinine), respectively. Brain ultrasound demonstrated cystic necrosis of the germinal matrix (extensive symmetrical caudothalamic germinolysis) and mild striatal arteriopathy. The child died of respiratory and multiple organ failure at 5 days of age. Measurement of respiratory-chain activity in fibroblasts demonstrated decreased complex IV activity. Additional clinical descriptions and experimental details are provided in the Supplemental Note.

Written informed consent was obtained from the parents, and investigations were performed according to the regional ethics committees at the Karolinska Institutet (Sweden), the Saitama Medical University (Japan), and Antwerp University Hospital (Belgium).

Homozygosity mapping, exome sequencing,<sup>5–11</sup> and Sanger confirmation (Figures 1A and 1B and Figure S2A) revealed *SLC25A26* mutations (GenBank: NM\_173471.3) in all affected individuals and their parents. We identified conserved missense mutations in P1, homozygous for a c.443T>C (p.Val148Gly) substitution, and P2, compound heterozygous for c.305C>T (p.Ala102Val) and c.596C>T (p.Pro199Leu). P3 was homozygous for a splice mutation (c.33+1G>A) (Figure 1C), which results in either a frameshift mutation in *SLC25A26*, when an alternative splice site in exon 2 is used, or a shorter polypeptide lacking the first 88 amino acids (SAMCΔ1–88), as a result of an alternative translation initiation site in exon 4 (Figure S2B). Cloning and sequencing of cDNA from P3 fibroblasts of this region confirmed the presence of exclusively alternative splice variants (Figure S2C). The shortened transcript lacks the first two transmembrane helices (Figure S3) and failed to co-localize (Figure 1D) or be detected in mitochondria by western blot analysis (Figure 1E), indicating that it does not encode a functional mitochondrial carrier protein. Additionally, the splice mutation resulted in reduced *SLC25A26* mRNA transcript levels in fibroblasts from P3, whereas P1 and P2 samples were unaffected (Figure 1F).

The conservation of all three missense mutations among 87 species (Ala102 [84%], Val148 [100%, including Leu and Ile], and Pro199 [100%]) suggests that their replacement might disrupt protein function. We also considered the transversal scores of the altered SAMC residues (these scores are a measure of the strength of the evolutionary selection acting on the residues) from a study of the rate of single-nucleotide evolution.<sup>12</sup> These values (4.52 for Ala102, 3.68 for Val148, and 5.15 for Pro199) are all close to or greater than 3.7, previously shown to represent sites of functional importance in mitochondrial carriers.<sup>12</sup> Furthermore, the position of all three *SLC25A26* missense mutations in the structural homology model

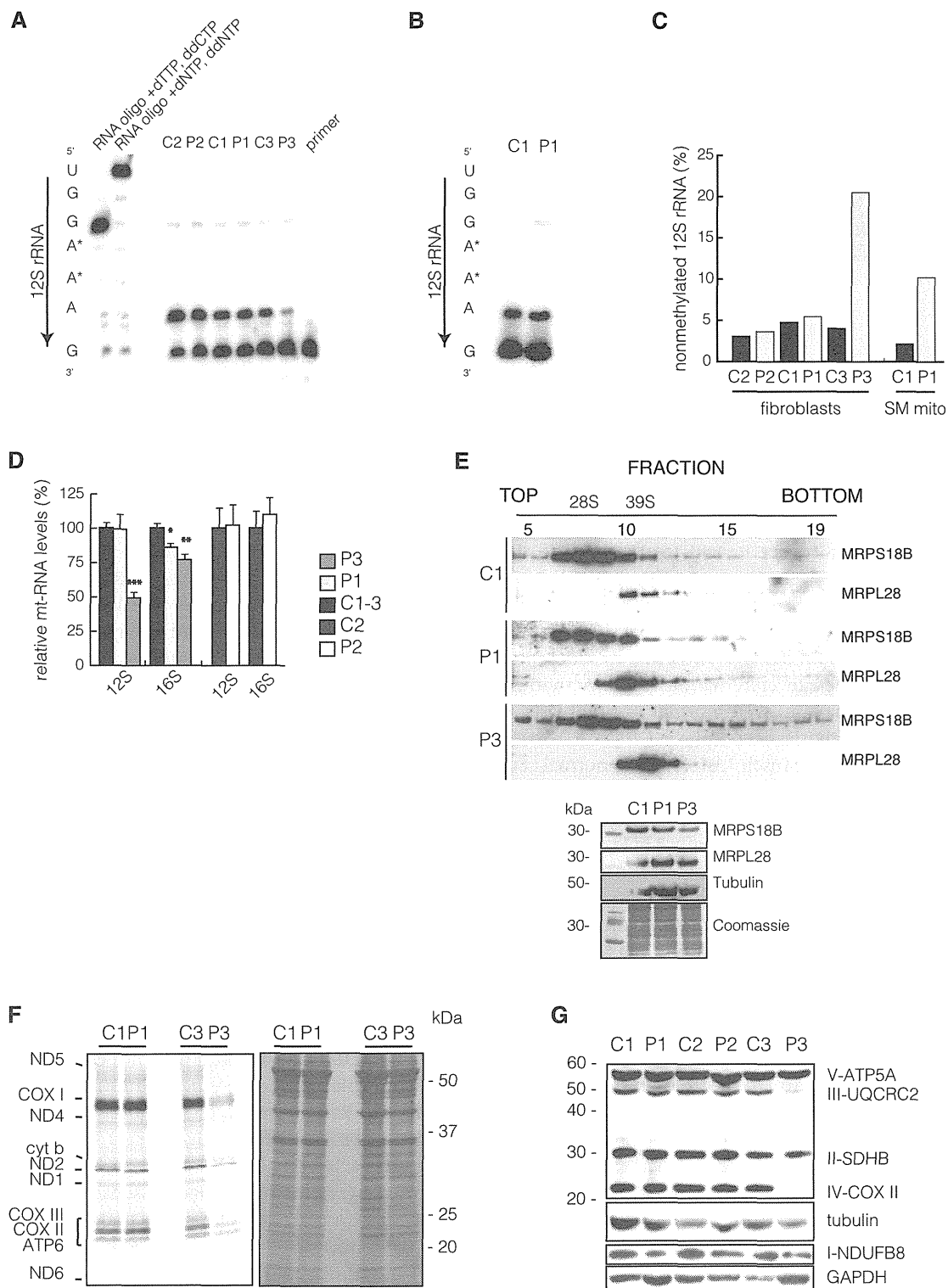


**Figure 3. Affected Mitochondrial Translation**

(A and B) Poisoned primer extension on total RNA from (A) fibroblasts or (B) skeletal-muscle mitochondria and subsequent size separation by denaturing PAGE. [<sup>32</sup>P] end-labeled oligo complement to the 3' terminus of 12S rRNA was annealed to RNA extracts and elongated in the presence of dTTP and ddCTP by M-MLV reverse transcriptase. In the case of adenine dimethylation, reverse transcription will terminate upstream of the dimethylation, whereas in its absence, termination will occur immediately downstream of the first guanidine residue because of ddCTP.

(C) Quantification of termination and read-through of (A) and (B).

(D) qRT-PCR of the steady-state levels of 12S and 16S rRNA in fibroblasts. The mean value of two independent experiments performed in triplicate is shown.

(legend continued on next page)

of SAMC also suggested a pathogenic effect of the mutations (Figure S4).<sup>13</sup> We confirmed pathogenicity by complementation studies in an *S. cerevisiae* SAMC-null strain (SAM5Δ)<sup>14</sup> by revealing that the growth phenotype of SAM5Δ cells on non-fermentable carbon sources could not be restored by complementation of the knockout strain with the p.Ala102Val, p.Pro199Leu, or SAMCΔ1–88 variant. Only the p.Val148Gly altered SAMC partially rescued the growth defect of SAM5Δ cells (Figure 2A). Additionally, we measured SAM transport capacity in reconstituted liposomes as previously described<sup>15–19</sup> and demonstrated a severe abrogation of SAM transport capacity for all altered proteins (Figures 2B and 2C and Figure S5). SAMCΔ1–88 was completely inactive, whereas p.Ala102Val and p.Pro199Leu variants exhibited negligible activity, and p.Val148Gly strongly inhibited SAMC activity (15% of wild-type SAMC). All together, conservation scores, yeast complementation, and in vitro reconstitution studies confirm the deleterious consequences of the *SLC25A26* mutations on SAMC function. Also supporting this is that the various degrees of residual SAM-import capacity correlated well with the severity of the clinical presentation and biochemical phenotype in the affected individuals.

Methylation is required for a multitude of mitochondrial processes, including RNA and protein modifications, and we therefore investigated the status of adenine dimethylation in the hairpin loop at the 3' end of the mitochondrial 12S rRNA by poisoned primer extension,<sup>20</sup> known to be methylated via mtSAM.<sup>21–23</sup> In control samples, the majority of 12S rRNA molecules were dimethylated at adenines 936–937, whereas fibroblasts from P3 (Figure 3A) and skeletal-muscle mitochondria from P1 (Figure 3B) revealed a substantial shift from methylated to non-methylated ribosomal transcripts (Figure 3C). Surprisingly, not only did we fail to observe a methylation defect in fibroblast samples from individuals P1 and P2, but there was also substantial termination of primer extension in P3 fibroblasts, suggesting some methylation of 12S rRNA despite the complete lack of SAMC activity. 12S rRNA steady-state levels are dependent on adenine dimethylation,<sup>23</sup> and in agreement with this, 12S rRNA steady-state levels in fibroblasts from P3 were decreased (Figure 3D), whereas all other transcripts tested had only mild changes (Figures S6A and S6B). Additionally, mitochondrial ribosomal assembly was only moderately affected in P3, who showed reduced amounts of the small and possible stabilization of the large mitochondrial ribosome subunits (Figure 3E). Despite the

mild effect on mitochondrial ribosome assembly, de novo mitochondrial translation<sup>25</sup> was severely affected in P3 fibroblasts (Figure 3F), possibly because methylation is required for tRNA maturation. This defect is also reflected by the reduced steady-state level of COXII (Figure 3G), a subunit of complex IV, and most likely contributes to the mitochondrial dysfunction in P1 skeletal muscle, which showed reduced levels of complexes I and IV (Figure S1).

Several mitochondrial proteins are known to be methylated by S-adenosylmethionine-dependent methyltransferases.<sup>26,27</sup> We studied the methylation status of three known mitochondrial SAM targets, ADP/ATP translocators ANT1 and ANT2, and the electron-transferring flavoprotein ETFB. Western blot analysis against di- and tri-methyl lysine (DTML) revealed decreased methylation levels in all fibroblast samples from affected individuals, and P3 was the most severely affected (Figure 4A). Transfection of cell lines from affected individuals with exogenous ANT1 and ANT2 further confirmed the methylation deficiency (Figure 4B). Loss of protein methylation was further rescued by wild-type SAMC in fibroblasts from P2 and P3 (Figure 4C).

Lipoic acid (LA) metabolism depends heavily on SAM-dependent methylation within mitochondria.<sup>31</sup> Individual P1 presented with high plasma glycine and low ATP production in muscle when pyruvate was used as a substrate, consistent with deficiencies of the glycine cleavage system and the pyruvate dehydrogenase complex, both of which require LA. These measurements were not performed for individual P2 or P3. Fibroblasts from individuals P1–P3 showed reduced levels of the LA subunits pyruvate dehydrogenase complex E2 (PDHC-E2) and alpha-ketoglutarate dehydrogenase E2 ( $\alpha$ -KGDH-E2) (Figures 4D and 4E), and P3 was the most severely affected. This decrease was not secondary to the mitochondrial dysfunction observed, given that two independent samples from individuals with unrelated mitochondrial diseases showed normal levels of LA (M1 and M2 in Figure 4E), whereas samples from individuals with mutations affecting LA biosynthesis were severely reduced (B1–B4 in Figure 4E).

The final steps of coenzyme Q<sub>10</sub> (CoQ<sub>10</sub>) biosynthesis, including several methylation steps of the benzoquinone ring, are performed within the mitochondrial network.<sup>32</sup> We therefore measured CoQ<sub>10</sub> levels in isolated skeletal-muscle mitochondria from P1 as previously described<sup>7,28</sup> and observed that they were severely decreased, presumably as a result of impaired CoQ<sub>10</sub> biosynthesis (Figure 4F). In order to investigate the bioenergetic

(E) Ribosomal gradients (top panel) from fibroblast mitochondria of P1 and P3. Ribosomes were separated in 10%–30% sucrose gradient by centrifugation and then fractionated as previously described,<sup>24</sup> with slight modifications. Western blot analysis against subunits of the small ribosomal subunit (28S; MRPS18B) or large subunit (39S; MRPL28) revealed their individual migration and ribosomal monosome (55S) formation. Loading onto the gradient was controlled by input western blot analysis (bottom panel) against mtSSU (MRPS18B), mt-LSU (MRPL28), and tubulin. Additionally, a Coomassie stain is shown.

(F) For determining de novo translation,<sup>25</sup> fibroblasts were cultured for 45 min in the presence of [<sup>35</sup>S] methionine and cysteine; then, protein extracts were separated by SDS-PAGE, and the gel was exposed. The low-molecular-weight subunits of ND3, ATP8, and ND4L are not shown.

(G) Western blot analysis of fibroblasts used antibodies against nuclear-encoded subunits of complexes I–V.

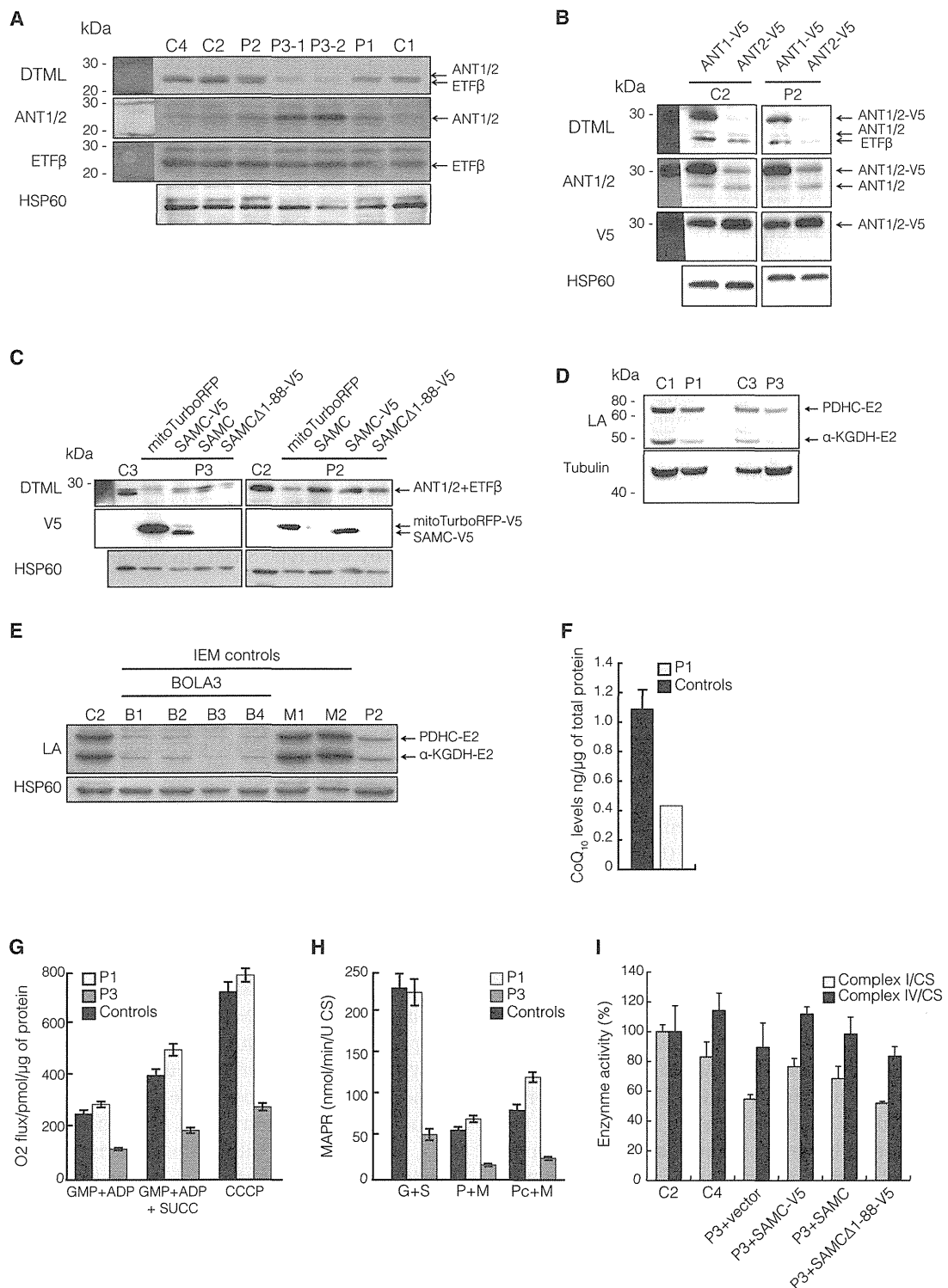


**Figure 4. Effects of Reduced Mitochondrial Methylation**

(A) Steady-state levels of ANT1, ANT2, and ETFβ (middle panels) in individuals P1–P3 and control cells (C1, C2, and C4), as well as DTML levels (upper panel) normalized to HSP60.

(B) Control (C2) or P2 fibroblasts were transfected with V5-tagged isoforms of ANT (ANT1-V5 and ANT2-V5) for determining DTML methylation of ANT1-V5 and ANT2-V5.

(C) Western blot analysis of DTML levels in samples from control (C2 and C3) and P2 and P3 fibroblasts transfected with empty vector (mitoTurboRFP), wild-type SAMC (SAMC), V5-tagged SAMC (SAMC-V5), or the N-terminal-truncated SAMC (SAMCΔ1-88-V5).

(D and E) Western blot analysis of the lipoic acid (LA) subunits pyruvate dehydrogenase complex E2 (PDHC-E2) and alpha-ketoglutarate dehydrogenase E2 (α-KGDH-E2) in (D) control (C1 and C3) and P1 and P3 samples or in (E) control (C2) or affected (B1–B4, M1 and M2,

(legend continued on next page)

consequences of reduced mtSAM import, we measured both oxygen consumption (Figure 4G) and mitochondrial ATP production rates (Figure 4H) in fibroblasts carrying the mildest (P1) or null (P3) mutations. Fibroblasts from P3 showed reduced oxygen consumption (Figure 4G) and reduced mitochondrial ATP production rates (Figure 4H), whereas P1 fibroblasts, in contrast to muscle samples (Figure S1A), showed no defect. Finally, the biochemical defects of P3 fibroblasts in the activity of complexes I and IV was rescued by transiently expressing wild-type and tagged wild-type SAMC, but not SAMCΔ1–88 (Figure 4I).

In summary, we have presented three individuals affected by a primary defect in the mitochondrial methylome. Our results show that impaired SAM transport into mitochondria causes a complex syndrome causing multiple primary defects, including those affecting RNA stability, protein modification, mitochondrial translation, and the biosynthesis of CoQ<sub>10</sub> and LA. We identified three individuals who originate from different ethnic groups and share striking similarities both biochemically and clinically, consistent with the degree of residual SAM-import capacity. Surprisingly, even though we studied SAMC-null samples, we detected some degree of intra-mitochondrial methylation, suggesting that other forms of methylation or recycling of methyl groups originating from imported methylated proteins might occur within mitochondria.

### Supplemental Data

Supplemental Data include a Supplemental Note and six figures and can be found with this article online at <http://dx.doi.org/10.1016/j.ajhg.2015.09.013>.

### Acknowledgments

We thank the families who participated in this study; Y. Mogami, K. Tominaga, Y. Tokuzawa, H. Nyuzuki, Y. Yatsuka, S. Tamaru, C. Shimizu, and S. Suzuki for technical assistance; and H. Miyoshi of Keio University and RIKEN BioResource Center for the CS-CA-MCS plasmid. This work was supported by the Japanese Ministry of Education, Culture, Sports, Science, and Technology (Innova-

tive Cell Biology by Innovative Technology and Strategic Research Centers at private universities) and the Takeda Science Foundation to Y.O.; Japan Society for the Promotion of Science KAKENHI 20634398 to Y.K.; Research on Intractable Diseases (Mitochondrial Disorder) from the Ministry of Health, Labor, and Welfare of Japan to A.O.; and Grants-in-Aid for the Practical Research Project for Rare/Intractable Diseases from the Japan Agency for Medical Research and Development to K.M. Support was also given by the Swedish Research Council (A. Wedell [VR12198]; A. Wredenberg [VR521-2012-2571]); Karolinska Institutet (A. Wredenberg [2013fobi38557]; C.F. [2013fobi37932]); Åke Wiberg Foundation (A. Wredenberg [738762088]; C.F. [367990950]); Stockholm County Council (A. Wedell [20140053]; A. Wredenberg [K0176-2012]); Swedish Foundation for Strategic Research (A. Wredenberg [ICA 12-0017]); and Knut & Alice Wallenberg Foundation (A. Wedell and A. Wredenberg [KAW 20130026]). A. Wredenberg is a Ragnar Söderberg fellow (M77/13). F.P. received grants from the Comitato Telethon Fondazione Onlus (GGP11139) and Italian Human ProteomeNet (RBRNO7BMCT-009). B.L.L. is a senior clinical investigator of the Fund for Scientific Research, Flanders (FWO, Belgium), holds a European Research Council (ERC) starting grant, and received additional support from the FWO (G.0221.12) and ERC.

Received: August 14, 2015

Accepted: September 29, 2015

Published: October 29, 2015

### Web Resources

The URLs for data presented herein are as follows:

OMIM, <http://www.omim.org>

RefSeq, <http://www.ncbi.nlm.nih.gov/refseq/>

### References

1. Carrasco, M., Rabaneda, L.G., Murillo-Carretero, M., Ortega-Martínez, S., Martínez-Chantar, M.L., Woodhoo, A., Luka, Z., Wagner, C., Lu, S.C., Mato, J.M., et al. (2014). Glycine N-methyltransferase expression in the hippocampus and its role in neurogenesis and cognitive performance. *Hippocampus* 24, 840–852.
2. Infantino, V., Castegna, A., Iacobazzi, F., Spera, I., Scala, I., Andria, G., and Iacobazzi, V. (2011). Impairment of methyl

and P2) samples. Control samples were obtained from individuals with non-related inborn errors of metabolism (IEMs) and either mutations in *BOLA3* (Bola family member 3) (B1–B4) or unrelated mitochondrial diseases (M1 and M2).

(F) CoQ<sub>10</sub> levels in mitochondrial extracts from skeletal muscle were determined by ultra-performance liquid chromatography tandem mass spectrometry<sup>7,28</sup> in four control samples (black) and muscles from affected individuals (gray). Control values are the mean ± SD of four control samples.

(G) Mitochondrial oxygen consumption of control (black) or P1 and P3 (gray) fibroblasts. Measurements were performed on an Oroboros oxygraph in the presence of (left) complex I substrates glutamate, malate, pyruvate (GMP), and ADP; (middle) complex I and II substrates GMP, succinate, and ADP; or (right) complex I and II substrates GMP, ADP, succinate, and the mitochondrial uncoupler carbonyl cyanide *m*-chlorophenyl hydrazone (CCCP). Error bars indicate the SEM of three independent experiments.

(H) Mitochondrial ATP production rate (MAPR)<sup>29</sup> in control (C1–C3; black) and P1 and P3 (gray) fibroblasts was determined by a firefly-luciferase-based method using glutamate and succinate (G+S), pyruvate and malate (P+M), or palmitoyl-L-carnitine and malate (Pc+M) as a substrate at 25°C. Results are presented as the ATP synthesis rate (units) per unit of citrate synthase (CS) activity. Values are the mean ± SEM of three independent experiments.

(I) Isolated enzyme activities<sup>29,30</sup> of complexes I (gray) and IV (black) are normalized to citrate synthase (CS) activities from control (C2 and C4) and P3 fibroblast cell lines after transfection with empty vector (mitoTurboRFP; P3), V5-tagged SAMC (SAMC-V5), SAMC, or V5-tagged SAMCΔ1–88.



- cycle affects mitochondrial methyl availability and glutathione levels in Down's syndrome. *Mol. Genet. Metab.* *102*, 378–382.
3. Clarke, S.G. (2013). Protein methylation at the surface and buried deep: thinking outside the histone box. *Trends Biochem. Sci.* *38*, 243–252.
  4. Agrimi, G., Di Noia, M.A., Marobbio, C.M.T., Fiermonte, G., Lasorsa, F.M., and Palmieri, F. (2004). Identification of the human mitochondrial S-adenosylmethionine transporter: bacterial expression, reconstitution, functional characterization and tissue distribution. *Biochem. J.* *379*, 183–190.
  5. Stranneheim, H. (2014). Mutation Identification Pipeline (MIP), <https://github.com/henrikstranneheim/MIP>.
  6. Stranneheim, H., Engvall, M., Naess, K., Lesko, N., Larsson, P., Dahlberg, M., Andeer, R., Wredenberg, A., Freyer, C., Barbaro, M., et al. (2014). Rapid pulsed whole genome sequencing for comprehensive acute diagnostics of inborn errors of metabolism. *BMC Genomics* *15*, 1090.
  7. Freyer, C., Stranneheim, H., Naess, K., Mourier, A., Felser, A., Maffezzini, C., Lesko, N., Bruhn, H., Engvall, M., Wibom, R., et al. (2015). Rescue of primary ubiquinone deficiency due to a novel COQ7 defect using 2,4-dihydroxybenzoic acid. *J. Med. Genet.* Published online June 17, 2015. <http://dx.doi.org/10.1136/jmedgenet-2015-102986>.
  8. Ohtake, A., Murayama, K., Mori, M., Harashima, H., Yamazaki, T., Tamaru, S., Yamashita, Y., Kishita, Y., Nakachi, Y., Kohda, M., et al. (2014). Diagnosis and molecular basis of mitochondrial respiratory chain disorders: exome sequencing for disease gene identification. *Biochim. Biophys. Acta* *1840*, 1355–1359.
  9. Haack, T.B., Jackson, C.B., Murayama, K., Kremer, L.S., Schaller, A., Kotzaeridou, U., de Vries, M.C., Schottmann, G., Santra, S., Büchner, B., et al. (2015). Deficiency of ECHS1 causes mitochondrial encephalopathy with cardiac involvement. *Ann. Clin. Transl. Neurol.* *2*, 492–509.
  10. Scharpf, R.B., Parmigiani, G., Pevsner, J., and Ruczinski, I. (2008). Hidden Markov models for the assessment of chromosomal alterations using high-throughput SNP arrays. *Ann. Appl. Stat.* *2*, 687–713.
  11. Vandeweyer, G., Reyniers, E., Wuyts, W., Rooms, L., and Kooy, R.F. (2011). CNV-WebStore: online CNV analysis, storage and interpretation. *BMC Bioinformatics* *12*, 4.
  12. Pierri, C.L., Palmieri, F., and De Grassi, A. (2014). Single-nucleotide evolution quantifies the importance of each site along the structure of mitochondrial carriers. *Cell. Mol. Life Sci.* *71*, 349–364.
  13. Palmieri, F. (2013). The mitochondrial transporter family SLC25: identification, properties and physiopathology. *Mol. Aspects Med.* *34*, 465–484.
  14. Marobbio, C.M.T., Agrimi, G., Lasorsa, F.M., and Palmieri, F. (2003). Identification and functional reconstitution of yeast mitochondrial carrier for S-adenosylmethionine. *EMBO J.* *22*, 5975–5982.
  15. Palmieri, F., Indiveri, C., Bisaccia, F., and Iacobazzi, V. (1995). Mitochondrial metabolite carrier proteins: purification, reconstitution, and transport studies. *Methods Enzymol.* *260*, 349–369.
  16. Capobianco, L., Bisaccia, F., Mazzeo, M., and Palmieri, F. (1996). The mitochondrial oxoglutarate carrier: sulfhydryl reagents bind to cysteine-184, and this interaction is enhanced by substrate binding. *Biochemistry* *35*, 8974–8980.
  17. Palmieri, L., De Marco, V., Iacobazzi, V., Palmieri, F., Runswick, M.J., and Walker, J.E. (1997). Identification of the yeast ARG-11 gene as a mitochondrial ornithine carrier involved in arginine biosynthesis. *FEBS Lett.* *410*, 447–451.
  18. Palmieri, L., Arrigoni, R., Blanco, E., Carrari, F., Zanor, M.L., Studart-Guimaraes, C., Fernie, A.R., and Palmieri, F. (2006). Molecular identification of an Arabidopsis S-adenosylmethionine transporter. Analysis of organ distribution, bacterial expression, reconstitution into liposomes, and functional characterization. *Plant Physiol.* *142*, 855–865.
  19. Palmieri, F., and Klingenberg, M. (1979). Direct methods for measuring metabolite transport and distribution in mitochondria. *Methods Enzymol.* *56*, 279–301.
  20. Rio, D.C., Ares, M., Hannon, G.J., and Nilsen, T.W. (2011). RNA: A Laboratory Manual (Cold Spring Harbor Laboratory Press).
  21. Helser, T.L., Davies, J.E., and Dahlberg, J.E. (1971). Change in methylation of 16S ribosomal RNA associated with mutation to kasugamycin resistance in *Escherichia coli*. *Nat. New Biol.* *233*, 12–14.
  22. Poldermans, B., Van Buul, C.P., and Van Knippenberg, P.H. (1979). Studies on the function of two adjacent N6,N6-dimethyladenosines near the 3' end of 16 S ribosomal RNA of *Escherichia coli*. II. The effect of the absence of the methyl groups on initiation of protein biosynthesis. *J. Biol. Chem.* *254*, 9090–9093.
  23. Metodieff, M.D., Lesko, N., Park, C.B., Cámara, Y., Shi, Y., Wibom, R., Hultenby, K., Gustafsson, C.M., and Larsson, N.-G. (2009). Methylation of 12S rRNA is necessary for in vivo stability of the small subunit of the mammalian mitochondrial ribosome. *Cell Metab.* *9*, 386–397.
  24. Rorbach, J., Boesch, P., Gammage, P.A., Nicholls, T.J.J., Pearce, S.F., Patel, D., Hauser, A., Perocchi, E., and Minczuk, M. (2014). MRM2 and MRM3 are involved in biogenesis of the large subunit of the mitochondrial ribosome. *Mol. Biol. Cell* *25*, 2542–2555.
  25. Leary, S.C., and Sasarman, F. (2009). Oxidative phosphorylation: synthesis of mitochondrially encoded proteins and assembly of individual structural subunits into functional holoenzyme complexes. *Methods Mol. Biol.* *554*, 143–162.
  26. Rhein, V.F., Carroll, J., Ding, S., Fearnley, I.M., and Walker, J.E. (2013). NDUFAF7 methylates arginine 85 in the NDUF52 subunit of human complex I. *J. Biol. Chem.* *288*, 33016–33026.
  27. Rhein, V.F., Carroll, J., He, J., Ding, S., Fearnley, I.M., and Walker, J.E. (2014). Human METTL20 methylates lysine residues adjacent to the recognition loop of the electron transfer flavoprotein in mitochondria. *J. Biol. Chem.* *289*, 24640–24651.
  28. Mourier, A., Motori, E., Brandt, T., Lagouge, M., Atanassov, I., Galinier, A., Rapp, G., Brodesser, S., Hultenby, K., Dieterich, C., and Larsson, N.G. (2015). Mitofusin 2 is required to maintain mitochondrial coenzyme Q levels. *J. Cell Biol.* *208*, 429–442.
  29. Wibom, R., Hagenfeldt, L., and von Döbeln, U. (2002). Measurement of ATP production and respiratory chain enzyme activities in mitochondria isolated from small muscle biopsy samples. *Anal. Biochem.* *311*, 139–151.
  30. Kirby, D.M., Thorburn, D.R., Turnbull, D.M., and Taylor, R.W. (2007). Biochemical assays of respiratory chain complex activity. *Methods Cell Biol.* *80*, 93–119.
  31. Booker, S.J., Cicchillo, R.M., and Grove, T.L. (2007). Self-sacrifice in radical S-adenosylmethionine proteins. *Curr. Opin. Chem. Biol.* *11*, 543–552.
  32. Laredj, L.N., Licitra, E., and Puccio, H.M. (2014). The molecular genetics of coenzyme Q biosynthesis in health and disease. *Biochimie* *100*, 78–87.



The American Journal of Human Genetics

Supplemental Data

## Intra-mitochondrial Methylation Deficiency

### Due to Mutations in *SLC25A26*

Yoshihito Kishita, Aleksandra Pajak, Nikhita Ajit Bolar, Carlo M.T. Marobbio, Camilla Maffezzini, Daniela V. Miniero, Magnus Monné, Masakazu Kohda, Henrik Stranneheim, Kei Murayama, Karin Naess, Nicole Lesko, Helene Bruhn, Arnaud Mourier, Rolf Wibom, Inger Nennesmo, Ann Jespers, Paul Govaert, Akira Ohtake, Lut Van Laer, Bart L. Loeys, Christoph Freyer, Ferdinando Palmieri, Anna Wredenberg, Yasushi Okazaki, and Anna Wedell

## Supplemental Note: case reports

The studies were approved by the regional Ethics Committees at Karolinska Institutet, Sweden, the Saitama Medical University, Japan and Antwerp University Hospital, Belgium. Written informed consent was obtained from the parents.

### **Individual 1**

Individual 1 (P1) was born 2009 in gestational week 39 to consanguineous healthy parents from Iraq. There is one healthy sister born 2006. Pregnancy and neonatal period were normal. Birth weight was 3360 grams, length 53 cm and head circumference 35.5 cm. The boy presented at 4 weeks with acute circulatory collapse and pulmonary hypertension, requiring extra-corporeal membrane oxygenation for 5 days. Urinary organic acid analysis showed increased excretion of lactate, 3-methyl-glutaconic acid and alpha-ketoglutarate but was otherwise normal. There was severe lactic acidosis around 20 mmol/L (ref 0.5-2.3). Sodium dichloroacetate had good effect, and the boy slowly normalized. Plasma lactate has since been intermittently slightly elevated but most often within the normal range. Plasma glycine was increased up to 617  $\mu\text{mol/L}$  (ref 80-320) at 5 weeks. Analyses of urinary amino acids, urinary purines and pyrimidines, and plasma acylcarnitines gave normal results.

A lung biopsy performed at 5 weeks showed slight interstitial oedema and muscularized arterioli compatible with pulmonary hypertension of unclear etiology, and discreet presence of hyperplastic pneumocytes and clear cells with increased glycogen, but no signs of capillary alveolar dysplasia, inflammation, or other abnormalities. Computer tomography (CT) of the chest and abdomen showed an enlarged right ventricle of the heart, wide *truncus pulmonalis* and prominent lung artery.

A muscle biopsy was performed at 8 weeks from the *tibialis anterior* muscle. Investigation of isolated muscle mitochondria revealed reduced activities of complex I and IV and reduced ATP production rate. In particular, ATP production was virtually absent using pyruvate as a substrate (Figure S1A and B). Gross muscle histology was unremarkable without any increase in centrally positioned nuclei and no signs of inflammation or increased glycogen content. There was an even ratio of type 1 and type 2 muscle fibres. Combined staining for SDH and COX revealed numerous COX-negative fibres (Figure S1C). There were no ragged red fibres and electron microscopy did not reveal any morphologically abnormal mitochondria. Blue native gel electrophoresis showed reduced amounts of complex I and IV of the respiratory chain (Figure S1D).

Sanger sequencing was performed of the complete mtDNA isolated from muscle and the *PDHA1*, *POLG*, and *TK2* genes from DNA isolated from blood, without positive findings.

At 3.5 years there was a second episode of pulmonary hypertension, which also normalized. An enlarged right atrium and ventricle of the heart was observed by echocardiogram. The boy was treated with sildenafil until 4 years 10 months of age. He has since been cardiopulmonary stable without this treatment.

At 6 years 3 months the boy has increasing muscle weakness, exercise intolerance and fatigue. He walks without support but only short stretches. He has severe problems with recurrent abdominal pain and lack of appetite, and development is slightly delayed.

### ***Individual 2***

Individual 2 (P2) was the first child of healthy Japanese parents. There is one healthy younger brother. The girl was born at 39 weeks of gestation. Her birth weight and height were 3076 g (+0.2 SD) and 48.2 cm (-0.7 SD). Apgar scores were 9 at 1 minute and 10 at 5 minutes. Around 11 hours after birth, she developed respiratory failure. Blood lactate was elevated at 41.8 mmol/L (ref <1.8) and showed severe acidosis (pH 6.6). Pyruvate levels were 0.65 mmol/L (ref <0.1). She required mechanical ventilation and peritoneal dialysis. Histology of a muscle biopsy specimen at 6 days indicated no ragged red fibers (RRF) but mild COX deficiencies were observed. There was no mutation in muscle mitochondrial DNA. Blood acylcarnitine analysis showed no abnormality. Urine organic acid analysis also showed no abnormality except for large amount of lactate. Amino acid profiles showed elevated alanine. At 133 days of age, she was discharged from hospital. Resting lactate levels in the blood was persistently high (4.4mmol/L) and acute infections caused an increase in blood lactate (>11.1mmol/L) despite treatment with vitamins, L-carnitine, coenzyme Q and dichloroacetic acid. She could walk at 1 year and her DQ score was 82 at 1 year and 10 months of age. When she was 2 years old, a remarkable hyperlacticacidemia (36.1 mmol/L) was observed, followed by cardiopulmonary arrest and hypoxic brain damage. After this episode she remained severely handicapped. A muscle biopsy was performed at 3 years and showed remarkable ragged RRF and COX deficiencies (Figure S1F). Respiratory chain enzyme activities were normal in fibroblasts but showed decreased complex I, III and IV activities in skeletal muscle (Figure S1E).

### ***Individual 3***

Individual 3 (P3), born to consanguineous parents of Moroccan decent, was delivered by caesarean section at 30 weeks 5 days after reduced fetal movements, polyhydramnios, fetal hydrops, and poor cardiotocography (CTG) were noted from 27 weeks of gestational age. She had normal antropometric parameters (birth weight 1300 grams, length 38 cm and head circumference 27.5 cm) but presented with poor Apgar score (3-5-6) due to bradycardia, hypotonia and respiratory insufficiency, necessitating assisted ventilation with high frequency oscillation. She suffered from lactic acidosis (84.6 mmol/L, ref 0.45-2.1 mmol/L) in CSF and urine (18 mmol/mmol creatinine, ref 1-285  $\mu$ mol/mmol creatinine) and had elevated pyruvate levels (1.2 mmol/mmol

creatinine, ref 1-130  $\mu\text{mol}/\text{mmol}$  creatinine) in urine. Brain ultra-sound demonstrated cystic necrosis of germinal matrix (extensive symmetrical caudothalamic germinolysis) and mild striatal arteriopathy. The child died of respiratory and multiple organ failure at 5 days of age. Measurement of respiratory chain activity in fibroblasts demonstrated decreased complex IV activity.